



TITLE:

The BcsD subunit of type I bacterial cellulose synthase interacts dynamically with the BcsAB catalytic core complex

AUTHOR(S):

Kondo, Tatsuya; Nakamura, Yui; Nojima, Shingo; Yao, Min; Imai, Tomoya

CITATION:

Kondo, Tatsuya ...[et al]. The BcsD subunit of type I bacterial cellulose synthase interacts dynamically with the BcsAB catalytic core complex. *FEBS Letters* 2022, 596(23): 3069-3086

ISSUE DATE:

2022-12

URL:

<http://hdl.handle.net/2433/277819>

RIGHT:

© 2022 The Authors. *FEBS Letters* published by John Wiley & Sons Ltd on behalf of Federation of European Biochemical Societies.; This is an open access article under the terms of the Creative Commons Attribution License, which permits use, distribution and reproduction in any medium, provided the original work is properly cited.

RESEARCH ARTICLE

The BcsD subunit of type I bacterial cellulose synthase interacts dynamically with the BcsAB catalytic core complex

Tatsuya Kondo^{1,*} , Yui Nakamura², Shingo Nojima², Min Yao²  and Tomoya Imai¹ 

1 Research Institute for Sustainable Humanosphere (RISH), Kyoto University, Japan

2 Faculty of Advanced Life Science, Hokkaido University, Sapporo, Japan

Correspondence

T. Imai, Research Institute for Sustainable Humanosphere (RISH), Kyoto University, Gokasho, Uji, Kyoto 611-0011, Japan
Tel: +81 774 38 3631
E-mail: imai.tomoya.4c@kyoto-u.ac.jp

M. Yao, Faculty of Advanced Life Science, Hokkaido University, N10W8 Kita-ku, Sapporo 060-0810, Japan
Tel: +81 11 706 4481
E-mail: yao@castor.sci.hokudai.ac.jp

*Present address

Institute of Fruit Tree and Tea Science, National Agriculture and Food Research Organization (NARO), Tsukuba, Japan

(Received 20 June 2022, revised 23 August 2022, accepted 24 August 2022, available online 26 September 2022)

doi:10.1002/1873-3468.14495

Edited by Ulf-Ingo Flügge

Cellulose synthase has two distinct functions: synthesis of the cellulose molecule (polymerization) and assembling the synthesized cellulose chains into the crystalline microfibril (crystallization). In the type I bacterial cellulose synthase (Bcs) complex, four major subunits – BcsA, BcsB, BcsC and BcsD – work in a coordinated manner. This study showed that the crystallization subunit BcsD interacts with the polymerization complex BcsAB in two modes: direct protein–protein interactions and indirect interactions through the product cellulose. We hypothesized that the former and latter modes represent the basal and active states of type I bacterial cellulose synthase, respectively, and this dynamic behaviour of the BcsD protein regulates the crystallization process of cellulose chains.

Keywords: cellulose; cellulose synthase; membrane protein complex; protein–protein interaction

Cellulose is a natural polymer, whose molecular structure is composed of a homopolymer of glucose with a $\beta 1 \rightarrow 4$ linkage, which is very simple. The native elementary structure of cellulose is a long slender fibre in which cellulose molecules are packed in an extended chain conformation. This structural feature underlies the structure-sustaining property of cellulose, which many cellulose-producing organisms rely on.

This polymer assembly is produced by the enzyme ‘cellulose synthase’. In many known cases, *in vivo*

cellulose synthase is a protein complex with several polypeptide subunits. The most important subunit in this complex is glycosyltransferase, which is called CesA. The first structural biological study of the CesA protein was reported in 2013 for cellulose synthase from the bacterium *Rhodobacter* (currently *Cereibacter*) *sphaeroides* [1,2], which has stimulated many biochemical studies on cellulose synthase.

Given its relative simplicity, bacterial cellulose synthase (Bcs) has been a good model in many studies on

Abbreviations

Bcs, bacterial cellulose synthase; c.v., column volume; CBB, Coomassie brilliant blue; CD, catalytic domain; c-di-GMP, cyclic-di-guanosine monophosphate; DDM, *n*-dodecyl- β -D-maltopyranoside; DGC, diguanylate cyclase; DP, degree of polymerization; FL, full length; GH, glycoside hydrolase; IMAC, immobilized metal affinity chromatography; PASC, phosphoric acid swollen cellulose; TBS, tris-buffered saline; TBS-T, tris-buffered saline with Tween-20; TPR, tetratricopeptide repeat.

cellulose synthase. Particularly, Bcs from bacteria belonging to the genus *Acetobacter*, some of which are currently named *Gluconacetobacter* or *Komagataeibacter* (the genus name ‘*Acetobacter*’ is used for these bacteria in this study), have been used extensively in studies. Although it is now known that many other bacteria produce cellulose, the function and structure of cellulose appear to vary with species [3]. For example, phosphoethanolamine cellulose has been reported in *Escherichia coli*, and this natural cellulose derivative is important for interacting with the host organism [4].

Among cellulose-synthesizing bacteria, *Acetobacter*, which has a gene cluster or operon categorized as type I [3], is characteristic of synthesizing highly crystalline cellulose microfibrils [5]. Previous studies have reported that the Bcs complex in *Acetobacter* is composed of at least four subunits [6,7] – BcsA (bacterial Cesa, catalytic subunit), BcsB (auxiliary subunit having a carbohydrate-binding domain and flavodoxin domain), BcsC (secretion of a glucan chain through the outer membrane) and BcsD (crystallization subunit). In addition, endoglucanase CMCax [8,9] [glycoside hydrolase family 8 (GH8)], unknown function protein Ccp [8,10] (also named as BcsH [3]) and β -glucosidase bglAx (GH3) [11] are considered to be functionally involved in the complex. Given that the cooperation of these subunits produces highly crystalline cellulose microfibrils, the spatial organization of these subunits in the cell is important for understanding the cellulose biosynthesis mechanism as a protein function [12].

In these subunits, the BcsD protein is found specifically in bacterial species producing highly crystalline cellulose microfibrils such as *Acetobacter* and *Asaia* [3,13,14], which possess a type I Bcs operon [3]. The *bcsD*-deficient mutant of *Acetobacter* showed a reduction in cellulose production, as well as a lack of the ability to synthesize crystalline cellulose microfibrils [6,7,15]. Sunagawa et al. [16] also demonstrated that BcsD interacts with Ccp (BcsH) in a pull-down assay. Given that the BcsD protein contains glucan chains inside its octamer structure [15], it has been proposed that BcsD is functionally located downstream of the BcsAB complex (the cellulose-polymerizing core of the Bcs complex [1,6,17,18]) [19,20]. Detailed information on how these functional units work together is key to understanding the mechanism by which cellulose synthase can bundle the synthesized glucan chains for spinning a long slender crystalline fibre at room temperature in an aqueous environment.

In this study, we analysed protein–protein interactions in the type I Bcs complex using the recombinant BcsABCD protein with the *E. coli* expression

system and clarified the interaction of BcsD with BcsAB complex as well as BcsC protein. One of the advantages of using recombinant proteins is that many mutant proteins are easily available [21]. Owing to this advantage, this study sheds light on the interaction between BcsAB and BcsD and demonstrates that there are two modes for this interaction: direct protein–protein interactions and indirect interactions through the cellulose molecules. We hypothesized that such bimodal interactions between BcsAB and BcsD proteins could be key to controlling cellulose synthesis dynamically *in vivo*.

Materials and methods

Chemicals

All chemicals used in this study were purchased from FUJIFILM Wako Pure Chemicals Co. Ltd. (Osaka, Japan), Nacalai Tesque Co. Ltd. (Kyoto, Japan) and Sigma-Aldrich Inc. (St. Louis, MO, USA), unless otherwise indicated.

Biological resources (1): cloning

Bcs genes (*bcsA*, *bcsB*, *bcsC* and *bcsD*) were prepared from genomic DNA extracted from cultured cells of *Komagataeibacter sucrofermentans* JCM9730, which was provided by the RIKEN BioResource Center (Tsukuba, Japan) and known by the strain name BPR2001 [22,23]. The endo- β 1,4-glucanase gene from *Bacillus subtilis* strain 168 (*bscel5A*) [24] was prepared from the genomic DNA provided by the American Type Culture Collection (ATCC23857D). The diguanylate cyclase gene (*dgc*) was identical to that used in our previous study [18]: tDGC from *Thermotoga maritima* MSB8 with a point mutation of R158A and truncation of the N-terminal 81 amino acid residues from V1 to V81 [25]. The gene for green fluorescent protein UV (GFPuv) [26] was prepared from the pGFPuv plasmid purchased from Takara Bio, Co. Ltd. (Shiga, Japan).

The cloning of these genes was performed by PCR using PrimeStarGXL (Takara Bio Co. Ltd.). Site-directed mutagenesis was performed by QuikChange II (Agilent Inc., Santa Clara, CA, USA) or the equivalent PCR-based method. The sequence of the PCR-amplified DNA was checked by the dye terminator method in a subcloning vector [pGEM-T easy (Promega Inc., Madison, WI, USA) or pTAC-2 (BioDynamics Laboratory Co. Ltd., Tokyo, Japan)], or final expression vector, which was performed at either of the Uji DNA-sequencing core (Kyoto University Research Administration Office) with an ABI Prism 310 Genetic Analyzer (Applied Biosystems Inc., Waltham, MA, USA), or Eurofins Genomics Inc. (Tokyo, Japan).

Biological resources (2): construction of the expression vectors

The protein expression vectors used in this study are summarized in Table 1. Expression vectors for BcsAB (BcsAB, BcsA^{D333N}B and BcsA^{W373A}B) were identical to those used

in previous studies [18,21]. The *bcsAB* gene in the operon form was inserted between the EcoRI and KpnI sites in pQE-80L (Qiagen, Hilden, Germany), and the upstream of the start codon was the original ribosomal binding site of *K. surofermentans* JCM9730.

Table 1. Experimental resources to express the proteins in this study. GOI, gene of interest.

Material	Source	Description	References
Bacterial cellulose synthase			
pQE-BcsAB [GOI was inserted between EcoRI and KpnI site in pQE-80L vector (Qiagen Inc.)]	LC428282 (<i>Komagataeibacter surofermentans</i> JCM9730)	Expression vector for BcsAB protein without tags	Imai et al. [18]
pQE-BcsA ^{D333N} B [GOI was inserted between EcoRI and KpnI site in pQE-80L vector (Qiagen Inc.)]	LC428282 (<i>Komagataeibacter surofermentans</i> JCM9730)	Expression vector for BcsAB protein with a catalytic-deficient point mutation of D333N, without tags	Sun et al. [21]
pQE-BcsA ^{W373A} B [GOI was inserted between EcoRI and KpnI site in pQE-80L vector (Qiagen Inc.)]	LC428282 (<i>Komagataeibacter surofermentans</i> JCM9730)	Expression vector for BcsAB protein with a catalytic-deficient point mutation of W373A, without tags	Sun et al. [21]
pQE-BcsABCD [GOI was inserted between EcoRI and HindIII site in pQE-80L vector (Qiagen Inc.)]	LC687564 (<i>Komagataeibacter surofermentans</i> JCM9730)	Expression vector for BcsABCD complex without tags	This study
pQE-BcsABCD _{H6} [GOI was inserted between EcoRI and HindIII site in pQE-80L vector (Qiagen Inc.)]	LC687564 (<i>Komagataeibacter surofermentans</i> JCM9730)	Expression vector for BcsABCD complex with hexahistidine tag at the C-terminal of BcsD protein	This study
pQE-BcsABC _{H6} D [GOI was inserted between EcoRI and HindIII site in pQE-80L vector (Qiagen Inc.)]	LC687564 (<i>Komagataeibacter surofermentans</i> JCM9730)	Expression vector for BcsABCD complex with hexahistidine tag at the N-terminal of BcsD protein	This study
pQE-BcsABCD _{GFPuvH6} [GOI was inserted between EcoRI and HindIII site in pQE-80L vector (Qiagen Inc.)]	LC687564 (<i>Komagataeibacter surofermentans</i> JCM9730)	Expression vector for BcsABCD complex with GFPuv followed by hexahistidine tag at the C-terminal of BcsD protein	This study
pQE-BcsA ^{D333N} B _{CDH6} [GOI was inserted between EcoRI and HindIII site in pQE-80L vector (Qiagen Inc.)]	LC687564 (<i>Komagataeibacter surofermentans</i> JCM9730)	Expression vector for BcsABCD complex with a catalytic-deficient point mutation of D333N introduced in BcsA; hexahistidine tag is fused to the C-terminal of BcsD protein	This study
pQE-BcsA ^{W373A} B _{CDH6} [GOI was inserted between EcoRI and HindIII site in pQE-80L vector (Qiagen Inc.)]	LC687564 (<i>Komagataeibacter surofermentans</i> JCM9730)	Expression vector for BcsABCD complex with a catalytic-deficient point mutation of W373A introduced in BcsA; hexahistidine tag is fused to the C-terminal of BcsD protein	This study
pET _{H6} BcsC _{TPRH6} [GOI was inserted between NdeI and XhoI site in pET28b (Merck Corp.)]	LC687564 (<i>Komagataeibacter surofermentans</i> JCM9730)	Expression vector for TPR domain of BcsC protein (Cys18–Gly848): hexahistidine-tag is fused to both N- and C-terminal of the protein	This study
pET-BcsD _{StreptII} [GOI was inserted between NcoI and HindIII site in pET28b vector (Merck Corp.)]	LC687564 (<i>Komagataeibacter surofermentans</i> JCM9730)	Expression vector for BcsD protein: Streptag(II) is fused to the C-terminal of BcsD protein	This study
Diguanylate cyclase (DGC)			
pBAD33et32-tDGC (Self-made vector in this study)	NP_229585 (<i>Thermotoga maritima</i> MSB8)	Expression vector of diguanylate cyclase with N-terminal truncation (K82 – S248) and a point mutation (R158A mutation): thioredoxin was fused to N-terminal end of the protein	This study

Table 1. (Continued).

Material	Source	Description	References
Cellulase			
pGEX-BsCel5A_FL [GOI was inserted between BamHI and XhoI site in pGEX4T-3 (Cytiva Inc.)]	Z29076 (<i>Bacillus subtilis</i> strain 168)	Expression vector for full-length endoglucanase protein from <i>Bacillus subtilis</i> (BsCel5A): signal peptide sequence (from Met1 to Ala28) was removed; GST tag is fused to the N-terminal of BsCel5A protein, which consists of glycoside hydrolase 5 domain (GH-5 domain, Ala29–Thr332) and carbohydrate-binding module (CBM-3 and Ile354–Asn499)	This study
pGEX-BsCel5A_CD [GOI was inserted between BamHI and XhoI site in pGEX4T-3 (Cytiva Inc.)]	Z29076 (<i>Bacillus subtilis</i> strain 168)	Expression vector for the catalytic domain (A29–T332) of BsCel5A: GST tag is fused to the N-terminal of the protein, which lacks the signal peptide sequence (Met1 – Ala28)	This study
pGEX-BsCel5A_FL ^m [GOI was inserted between BamHI and XhoI site in pGEX4T-3 (Cytiva Inc.)]	Z29076 (<i>Bacillus subtilis</i> strain 168)	Expression vector for full-length BsCel5A with activity-deficient double mutation (E169Q/E257Q): GST tag is fused to the N-terminal of the protein, which lacks the signal peptide sequence (Met1–Ala28)	This study
pGEX-BsCel5A_CD ^m [GOI was inserted between BamHI and XhoI site in pGEX4T-3 (Cytiva Inc.)]	Z29076 (<i>Bacillus subtilis</i> strain 168)	Expression vector for catalytic domain (A29–T332) of BsCel5A with activity-deficient double mutation (E169Q/E257Q): GST tag is fused to the N-terminal of the protein, which lacks the signal peptide sequence (Met1–Ala28)	This study

Expression vectors for BcsABCD (BcsABCD, BcsABC_{H6}D, BcsABC_{H6}, BcsA^{D333N}BCD_{H6}, BcsA^{W373A}BCD_{H6} and BcsABC_{GFPuvH6}) proteins were constructed from the vectors for BcsAB by inserting the *bcsABCD* gene in the operon form between the EcoRI and HindIII sites in pQE-80L. The ribosomal binding site in these BcsABCD expression vectors is exactly the same as that in the expression vectors of BcsAB, one of *K. sucrofermentans* JCM9730. DNA encoding the tag (hexahistidine or GFPuv) was added to *bcsD* during the PCR amplification.

The expression vectors for the TPR region of BcsC (BcsC_TPR: C18–G848) and BcsD were prepared for the pull-down assay. DNA-encoding hexahistidine tag was added to the 3'-end of the gene for BcsC_TPR during PCR amplification and inserted into the NdeI and XhoI sites in pET-28b (Merck Corp., Darmstadt, Germany) to express BcsC_TPR protein with dual hexahistidine tag at both N- and C-terminal –_{H6}BcsC_TPR_{H6}. DNA-encoding Streptag (II) was added to the 3'-end of the gene for BcsD and inserted between the NcoI and HindIII sites in pET28b to express BcsD with C-terminal Streptag(II)–BcsD_{StreptII}.

The gene for tDGC was inserted between the NdeI and HindIII sites in pBAD33et32, a customized plasmid DNA

in this study, to express the thioredoxin-fused tDGC protein to count the cellulose-synthesizing activity of the recombinant BcsAB and BcsABCD complex in our previous studies [18,21]. The detailed procedure for preparing pBAD33et32 is described in Appendix S1. Thioredoxin gene (*trx*) in pBAD33et32 was copied from pET32a (Merck Corp.) to replace the His-patch thioredoxin used in our previous study [18], which was derived from pBAD202-TOPO (Invitrogen Inc., Waltham, MA, USA).

For the bacterial endoglucanase gene *bcsE5A*, the putative signal peptide sequence (M1–A28) was removed from the full-length construct. Full-length (A29–N499) and catalytic domain (A29–T332) genes were inserted between BamHI and XhoI sites in pGEX4T-3 (Cytiva Inc., Marlborough, MA, USA) to express the N-terminal GST-fused endoglucanase BsCel5A.

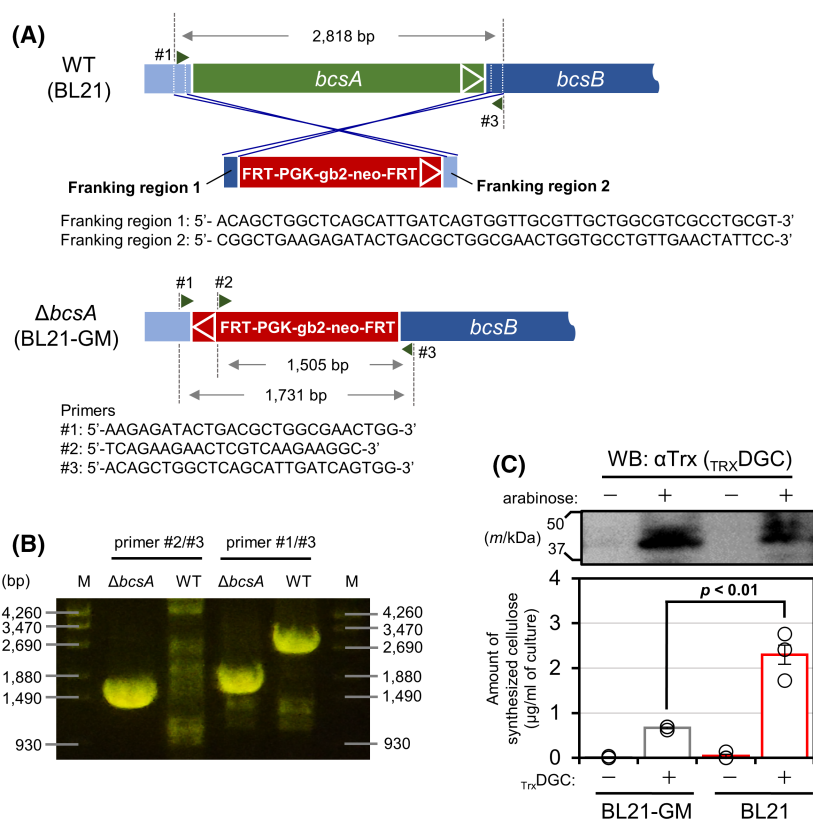
Biological resources (3): deletion of *bcsA* gene from *Escherichia coli* BL21

In this study, we used genetically modified *E. coli* BL21 to express Bcs proteins, which lack the whole *bcsA* gene (Fig. 1A). This gene manipulation was performed using the Red/ET recombination system (Gene Bridges GmbH,

T. Kondo et al.

BcsAB–BcsD interaction in type I bacterial cellulose synthase

Fig. 1. Deletion of the *E. coli* endogenous *bcsA* gene. (A) Schematic diagram of the experiment for deleting the endogenous *bcsA* gene using the Red/ET recombination system. The primer sequences used are listed in Table S1. (B) Electrophoresis pattern of colony-direct PCR using two pairs of primers. M: Molecular weight marker [Marker 6 (Nippon Gene Co. Ltd., Tokyo, Japan)]; $\Delta bcsA$: *bcsA*-deleted BL21; WT: wild-type BL21. (C) Quantification of endogenous cellulose synthesis in BL21-GM and BL21 cells. The CESEC system [18], which uses DGC expression to synthesize c-di-GMP to activate bacterial cellulose synthase, was used to count the amount of the synthesized cellulose (bottom). The expression of DGC was confirmed by western blot (WB) using an anti-Trx antibody (top). The experiments were performed in triplicate ($n = 3$) and are represented as mean \pm standard error of the mean (SEM), together with each of the data values. Statistical tests (Student's *t*-test) were performed using the built-in function in Microsoft Excel (TTEST).



Heidelberg, Germany), according to the manufacturer's specifications. The detailed procedure is described in Appendix S1.

Briefly, *E. coli* BL21 strain (purchased from New England Labs Inc., Ipswich, MA, USA) was transformed with the pRedET plasmid carrying the genes for DNA recombination proteins and selected by tetracycline resistance. The second transformation was followed by introducing linear DNA of the neomycin-resistant gene flanked by the homology arm sequences corresponding to the upstream and downstream of *bcsA* gene (CP010816.1); the proteins for homologous recombination were expressed with arabinose induction for disrupting *bcsA* gene, and subsequently, the pRedET plasmid was expelled out of the cell by culturing at 37 °C. Finally, the *bcsA*-disrupted BL21 transformant was selected for kanamycin resistance and tetracycline sensitivity. Gene modification was confirmed by direct PCR (Fig. 1B). We named this genetically modified *E. coli* BL21 strain as BL21-GM. Chemically competent cells of BL21-GM were then prepared by treating the cultured cells in a rubidium-based buffer according to the protocol on the website of the Center for Molecular Biology and Genetics at Mie University (<https://www.gene.mie-u.ac.jp/Protocol/Original/Transform-Comp-Cell-Freeze.html>, in Japanese).

In vivo cellulose synthase activity

The endogenous cellulose-synthesizing activity of *E. coli* and cellulose-synthesizing activity of the heterogeneously expressed Bcs complex in *E. coli* were estimated by expressing DGC protein to activate bacterial cellulose synthase in the cell by the produced c-di-GMP [18]. In this study, the pBAD33et32-tDGC plasmid was used to express the DGC. The obtained *E. coli* transformants were pre-cultured in LB medium including the proper antibiotics at 37 °C overnight, and then 0.1 mL of the pre-culture was inoculated into 10 mL of ZYP-5052 medium with 50 μ g·mL⁻¹ chloramphenicol (100 μ g·mL⁻¹ ampicillin when expressing Bcs complex) and 0.001% L-arabinose. Cells were grown at 20 °C with orbital shaking at 180 r.p.m. for 24 h and the cultured cells were collected by centrifugation at 2000 \times g for 20 min. The amount of cellulose in the pellet was quantified using the anthrone–sulfuric acid method [27] as described below.

Two millilitres of AN reagent (a mixture of glacial acetic acid and nitric acid with volumetric ratio of 8 : 1) was added to the pellet and then heated at 105 °C for 30 min. The remaining cellulose pellets were washed with 10 mL of water once by centrifugation at 2000 \times g for 10 min, and then 1 mL of 72% (v/v)

H₂SO₄ was added to the pellets and incubated for 1 h at room temperature. The solution (0.1 mL) was mixed with water (0.4 mL), and then, 1 mL of fresh anthrone reagent (0.2% w/v anthrone in concentrated H₂SO₄) was added and mixed. The solution was heated to 90 °C for 15 min and allowed to stand until it reached room temperature (approximately 15 min). The absorbance of the solution was measured at both 625 and 700 nm, and the absorbance at 625 nm, from which the absorbance at 700 nm was subtracted, was used for quantification for better reproducibility. Calibration was performed with phosphoric acid swollen cellulose (PASC) prepared using a previously reported protocol [28].

Purification and characterization of BsCel5A

Expression of GST-fused BsCel5A endoglucanase was performed in *E. coli* BL21 (not GM strain): all the four constructs (BsCel5A_FL, BsCel5A_CD, BsCel5A_FL^m and BsCel5A_CD^m) were expressed and purified in the same manner.

The transformant of BL21 with pGEX-BsCel5A was inoculated in 10 mL LB containing 100 µg·mL⁻¹ ampicillin in a 100 mL flask and grown at 37 °C with orbital shaking at 220 r.p.m. overnight. The cells were harvested by centrifugation at 3000 × *g* for 20 min, suspended in 1 L of LB containing 100 µg·mL⁻¹ ampicillin in a 5 L baffled flask and cultured at 37 °C until OD₆₀₀ reached 0.6. The culture medium was cooled in ice water for 10 min, and then IPTG was added to 0.1 mM and incubated at 20 °C for 20 h with orbital shaking at 160 r.p.m.

The cells were then collected at 3000 × *g* for 20 min, washed with 40 mL of 1 × phosphate-buffered saline (PBS), suspended in 40 mL of 1 × PBS containing 1 mM phenylmethylsulfonyl fluoride (PMSF) and sonicated on ice for ~5 min (exposure: 10 s and rest: 50 s; until slightly translucent). The cell lysate clarified by 20 000 × *g* for 30 min at 2 °C was applied to 5 mL of Glutathione Sepharose 4B (Cytiva Inc.), washed with 20 mL of 1 × PBS and eluted with 5 c.v. of 0.1 M Tris–HCl pH 8.0, 0.5 M NaCl and 20 mM reduced glutathione. The eluted fraction was buffer exchanged with 1 × PBS using Vivaspin 6 (MWCO 10 kDa; Sartorius AG, Germany).

To remove the GST tag fused to the N-terminus, 100 units of thrombin (Merck Corp.) was added to 10 mg of GSTBsCel5A and incubated at 20 °C for 2 days. Thrombin was then removed by adding 1 mL of Benzamidine Sepharose 6 B (Cytiva Inc.), and the cleaved GST was removed by adding 5 mL of Glutathione Sepharose 4 B. A solution of PMSF was added to the obtained BsCel5A protein at a final concentration of 1 mM to inactivate a small amount of residual thrombin.

The recombinant BsCel5A proteins purified were characterized with regard to the following points: (a) binding

activity to cellulose, (b) glycoside hydrolase activity and (c) substrate specificity. The detailed experimental procedure is described in Appendix S1.

Purification of BcsABCD complex

All the protein purification experiments in this study were performed at a low temperature (~4 °C). The composition of the protease inhibitor mix (PI) used for protein purification was as follows: 0.1 mM PMSF, 1 mM benzamidine-HCl, 5 µM bestatin, 10 µM leupeptin and 1 µM pepstatin A.

The transformant of *E. coli* BL21-GM with pQE-BcsABCD_{H6} was inoculated in 10 mL of LB containing 100 µg·mL⁻¹ ampicillin in a 100 mL flask and grown at 37 °C with shaking at 220 r.p.m. overnight. The cells were harvested by centrifugation at 3000 × *g* for 20 min, resuspended in 1 L of ZYP-5052 containing 100 µg·mL⁻¹ ampicillin and 0.0005% (v/v) antifoam SI (Fujifilm Wako Chemicals Co. Ltd., Osaka, Japan) in a 5 L baffled flask, and incubated at 20 °C for 22 h with an orbital shaker at 100 r.p.m. The cultured cells were collected at 3000 × *g* for 20 min and suspended in 50 mL of buffer A [20 mM sodium phosphate buffer (pH 7.5), 300 mM NaCl, 8% glycerol, 5 mM MgCl₂ and 5 mM cellobiose] with PI, prior to cell lysis by two passes of high-pressure homogenizer (French Press, Thermo Fisher Scientific Inc., Waltham, MA, USA) at a pressure of 15 000 psi. The lysate was clarified by centrifugation at 5000 × *g* for 10 min and ultracentrifugation at 150 000 × *g* for 30 min at 2 °C. The obtained cell membranes were resuspended in buffer A with PI and NaCl concentrations increased to 1 M and were ultracentrifuged again under the same conditions. Finally, the cell membrane was suspended in buffer A with PI to approximately 10 mg·mL⁻¹ (estimated by the DC protein assay, Bio-Rad Inc., Hercules, CA, USA). The collected cell membrane was stored at –80 °C until use in experiments.

Ten millilitres of the cell membrane suspension were mixed with *n*-dodecyl-β-D-maltopyranoside (DDM) at a final concentration of 0.5% (w/v) and shaken gently for 1 h at 4 °C for solubilizing Bcs-complex. The supernatant of the following ultracentrifugation at 150 000 × *g* for 30 min at 2 °C was collected as a solubilized fraction, and imidazole stock solution (2 M, pH 8.0) was added to achieve a final concentration of 10 mM prior to loading to 0.4 mL His-Select Cobalt Affinity Gel (Sigma-Aldrich Inc.), which was equilibrated with 4 mL of wash buffer [20 mM imidazole and 0.025% (w/v) DDM in buffer A] in advance. After loading the solubilized protein onto the affinity resin in a plastic open column, the resin in the column was washed with 3 mL of wash buffer and, finally, eluted with elution buffer [200 mM imidazole and 0.025% (w/v) DDM in buffer A].

Cellulase treatment of Bcs complex

Cellulase treatment of BcsABCD_{H6} was performed using a cobalt affinity gel. The same procedure was followed for the binding step of BcsABCD_{H6} on the affinity gel. After all the solubilized fractions passed through the column, 0.8 mL of 1.5 μM BscE5A solution in wash buffer [20 mM imidazole and 0.025% (w/v) DDM in buffer A] was loaded to the column. The column exit was plugged when most of the cellulase solution passed, and then the gel was incubated at 10 °C for 3 h with the remaining cellulase solution. After unplugging, the affinity gel in the column was washed with 2 mL of wash buffer and eluted with elution buffer [200 mM imidazole and 0.025% (w/v) DDM in buffer A].

Protein preparation for pull-down assay: BcsC_TPR, BcsD and crude BcsAB

The pull-down assay in this study used purified BcsC_TPR, purified BcsD and crude BcsAB proteins, each of which was prepared as described below.

The transformant of *E. coli* BL21(DE3) with pET-H₆BcsC_TPR_{H6} was inoculated in 10 mL of LB containing 50 μg·mL⁻¹ kanamycin in a 100 mL flask and grown at 37 °C with shaking at 220 r.p.m. overnight. The cells were harvested by centrifugation at 3000 × *g* for 20 min and resuspended in 1 L of ZYP-5052 [29] containing 200 μg·mL⁻¹ kanamycin and 0.0005% (v/v) antifoam SI in a 5 L baffled flask, and incubated at 20 °C for 24 h in a shaking incubator at 100 r.p.m. The cultured cells were collected at 3000 × *g* for 20 min, washed with 40 mL of 1 × PBS prior to resuspension in 100 mL of 10 mM imidazole in buffer B [20 mM sodium phosphate buffer (pH 7.5), 500 mM NaCl and 8% glycerol] with PI and sonicated on ice for ~ 5 min (exposure: 10 s and rest: 50 s; until slightly translucent). The cell lysate was clarified by centrifugation at 40 000 × *g* for 30 min at 2 °C and applied to 4 mL His-Select Cobalt Affinity Gel (Sigma-Aldrich Inc.), followed by washing with 10 mM imidazole in buffer B and eluted 250 mM imidazole in buffer B. Finally, the buffer of eluted fraction including H₆BcsC_TPR_{H6} protein was replaced with buffer B using PD-10 desalting column (Cytiva Inc.).

The BcsD protein was expressed in *E. coli* BL21(DE3) with pET-BcsD_{StrepII}. The transformant was inoculated in 10 mL of LB containing 50 μg·mL⁻¹ kanamycin in a 100 mL flask and grown at 37 °C with shaking at 220 r.p.m. overnight. The cells were harvested by centrifugation at 3000 × *g*, 20 min, resuspended in 1 L of LB containing 50 μg·mL⁻¹ kanamycin in a 5 L baffled flask and cultured at 37 °C until OD₆₀₀ was ~ 0.6. The culture medium was cooled in ice water for 30 min, and IPTG (0.5 mM) was added and incubated at 25 °C for 20 h at 120 r.p.m. Cells were collected at 3000 × *g* for 20 min, suspended in 30 mL of buffer C [20 mM Tris-HCl (pH 7.5),

150 mM NaCl and 1 mM EDTA] with PI and sonicated on ice for ~ 10 min (exposure: 10 s and rest: 50 s; until slightly translucent). The cell lysate was centrifuged at 20 000 × *g* for 30 min at 2 °C, applied to 2 mL of Streptactin Sepharose HP (Cytiva Inc.), washed with 20 mL of buffer C and eluted with 4 mM *d*-desthiobiotin in buffer C. Finally, a buffer of the eluted fraction was replaced by buffer C using Amicon Ultra-4 MWCO 50 kDa (Merck Corp.).

The crude protein of BcsAB was prepared using the transformant *E. coli* BL21-GM with pQE carrying the *bcsAB* gene. The procedure to isolate the cell membrane, from culture to ultracentrifugation, was the same as in the case of BcsABCD_{H6} as described previously, except for the buffer to suspend the cells and cell membrane: buffer D [20 mM sodium phosphate buffer (pH 7.5), 100 mM NaCl, 8% glycerol, 5 mM MgCl₂ and 5 mM cellobiose] with PI was used. The obtained cell membrane was suspended in buffer D with PI at approximately 10 mg·mL⁻¹ (estimated by the DC protein assay, Bio-Rad Inc.). Finally, crude BcsAB protein was prepared by solubilizing 7 mL of the cell membrane fraction with 0.5% (w/v) DDM for 1 h and centrifugation at 150 000 × *g* for 30 min at 2 °C.

Pull-down assays

For the pull-down by BcsD_{StrepII} with the crude BcsAB, purified BcsD_{StrepII} (0.2 mg) was added to 7 mL of crude BcsAB, incubated for 3 h at 4 °C and then loaded to 0.1 mL of Streptactin Sepharose HP. The resin was washed with 1 mL of 0.025% (w/v) DDM in buffer D, and finally, the bound protein was eluted with 4 mM desthiobiotin in buffer D with 0.025% (w/v) DDM.

For the pull-down assay, BcsD_{StrepII} with H₆BcsC_TPR_{H6} and BcsD_{StrepII} (0.1 mg) were incubated with H₆BcsC_TPR_{H6} (0, 0.1, 0.3 and 0.5 mg) in 3 mL of buffer D (-/-) (buffer D without MgCl₂ and cellobiose) for 3 h at 4 °C, and then loaded to 0.1 mL of Streptactin Sepharose HP. After washing with buffer D (-/-), the bound protein was eluted with 1 mL 4 mM *d*-desthiobiotin in buffer D (-/-).

For the pull-down assay by H₆BcsC_TPR_{H6} with BcsAB, purified H₆BcsC_TPR_{H6} (0.2 mg) was mixed with crude BcsAB (7 mL), and further NaCl stock solution was added to set 500 mM NaCl in the final solution. After incubation for 1 h at 4 °C, the sample was loaded to 0.2 mL His-Select Cobalt Affinity Gel and washed with 2 mL of 20 mM imidazole in buffer B (+/+) (buffer B with 5 mM MgCl₂ and 5 mM cellobiose) with 0.025% (w/v) DDM. The bound protein was eluted with 200 mM imidazole in buffer B containing 0.025% (w/v) DDM.

Finally, we performed a pull-down assay using BcsD_{StrepII}, purified BcsC_TPR, and crude BcsAB. BcsD_{StrepII} (0.2 mg) and H₆BcsC_TPR_{H6} (0.2 mg) were mixed with crude BcsAB (7 mL of DDM extract); NaCl stock solution (5 M) was added to a final concentration of 500 mM NaCl. After incubation for

3 h at 4 °C, the sample solution was loaded to 0.1 mL of Streptactin Sepharose HP. After washing with 1 mL of buffer B (+/+) containing 0.025% (w/v) DDM, the bound protein was eluted with 4 mM *d*-desthiobiotin in buffer B (+/+) containing 0.025% (w/v) DDM.

Prey protein without bait protein was used as a negative control for the pull-down assay using the same procedures. The eluted fraction was analysed by SDS/PAGE, followed by western blot as described in 2.4.6.

Western blot (WB) analysis

Rabbit polyclonal antibodies against BcsA, BcsB, BcsC and BcsD proteins were generated with the synthetic peptide corresponding to a part of the C terminus of BcsA [18,20,21,30], C terminus of BcsB (this study), C terminus of BcsC [30] and the loop between the β3 and β4 strand [20,30]. The dilution rate was 10 000-fold for anti-BcsA, anti-BcsB and anti-BcsC, whereas anti-BcsD was diluted 20 000-fold. Each of the antibodies against the peptide tag was diluted as follows: anti-Strep tag II (15 ng·mL⁻¹; ab180957, Abcam Corp., Cambridge, UK), anti-His5 (0.1 μg·mL⁻¹; 34660, Qiagen N.V.) and anti-Thioredoxin (1 μg·mL⁻¹; ab139677, Abcam Corp.).

Horseradish peroxidase (HRP)-conjugated anti-rabbit IgG (W401B; Promega Inc.) and HRP-conjugated anti-

mouse IgG (7076S; Cell Signaling Technology Inc., Danvers, MA, USA) were diluted 20 000-fold and used as the secondary antibodies. ECL-Prime (Cytiva Inc.) was used for chemical luminescence with HRP.

For the WB with anti-BcsD, anti-Strep, anti-His and anti-thioredoxin, the samples for SDS/PAGE were heat treated at 100 °C for 3 min after mixing with the sample buffer, while the samples to visualize by the other antibodies were incubated in the sample buffer for several minutes at room temperature. The samples were analysed by SDS/PAGE with a precast polyacrylamide gel (SuperSep Ace 5–20%, Fujifilm Wako Chemicals Co. Ltd.), and blotting from the gel to PVDF membrane (Immobilon-P, 0.45 μm-φ, Cytiva Inc.) was done by a constant current mode at 150 mA·10 cm⁻² for 30 min. Blocking of the membrane was performed with 0.3% skim milk and 0.02% NaN₃ in tris-buffered saline (TBS) containing 0.05% Tween-20 (TBS-T), for the WB with anti-Bcs proteins, while blocking was performed with 2.5% BSA, 0.1% gelatin, 0.02% Tween-20 and 0.04% NaN₃ in PBS at 4 °C overnight or at room temperature for 0.5–1 h, for anti-Strep-tag II, anti-His5 or anti-thioredoxin. The membranes were briefly rinsed with TBS-T and then subjected to the primary antibody reaction in blocking buffer for 1–2 h at room temperature. After removing the antibody solution, the membrane was briefly rinsed and washed with TBS-T

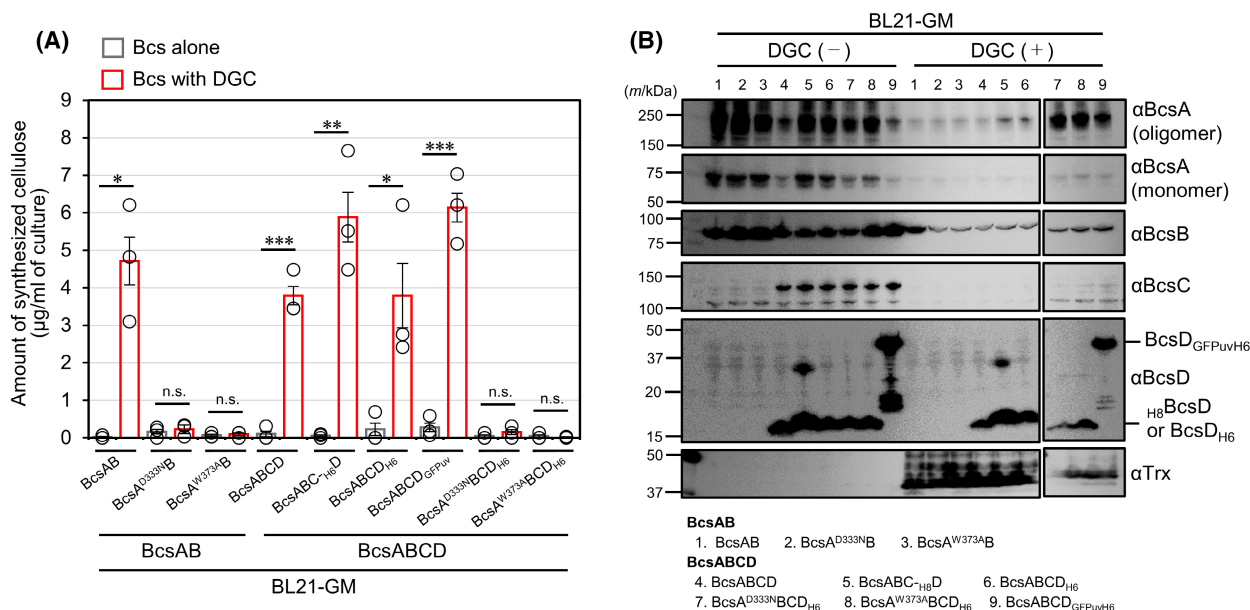


Fig. 2. *In vivo* cellulose-synthesizing activity of recombinant Bcs complex. (A) Cellulose-synthesizing activity of the recombinant Bcs complexes tested in this study: the amount of cellulose synthesized by the CESEC system [18] with BL21-GM ($\Delta bcsA$) is shown for each recombinant protein. All experiments were performed in triplicate ($n = 3$) and are represented as mean \pm SEM together with the significance of the difference between the expression of Bcs alone and the expression of Bcs with TRX-DGC: * for $P < 0.05$, ** for $P < 0.01$, *** for $P < 0.001$ and n.s. for not significant ($P > 0.1$) as a result of Student's *t*-test, which was performed using the built-in function of Microsoft Excel (TTEST). (B) WB was performed for the CESEC experiment to check the expression of BcsA, BcsB, BcsC, BcsD and TRX-DGC. Cultures with and without DGC expression were tested. For BcsA, the data are shown separately for the oligomer and monomer bands. Due to the limited number of wells in the SDS/PAGE gel, the gel was divided into two parts for electrophoresis.

thrice for 5 min, followed by a secondary antibody reaction in TBS-T for 30–45 min at room temperature. The membrane was briefly rinsed and washed with TBS-T three times for 15 min each time. The protein bands were then visualized by casting the ECL prime solution on the blotted PVDF membrane (0.2 mL·9 cm⁻² membrane) and digitally recorded with AE-9300H EZ-Capture MG (ATTO Co. Ltd., Taito, Japan).

Quantitative analysis was performed using IMAGEJ (National Institutes of Health, Bethesda, Maryland, USA, version 1.53a) to quantify the band signal intensity, calculated as relative values to the negative control and the relative signal intensities of BcsA and BcsB were normalized to the signal intensity of BcsD. For BcsA, two major bands were reproducibly observed near the 75- and 250-kDa marker (Fig. 2B, top row), as well as in our previous studies [18,30], which are probably BcsA monomer and BcsA-including oligomer, respectively (the estimated molecular weight for the BcsA monomer is 84 kDa). Given these observations, the band intensity for the BcsA-containing oligomer was also considered in addition to the monomer band intensity in subsequent analyses.

Results

Production of endogenous *bcsA* gene-deficient *E. coli*

This study analysed heterogeneously expressed Bcs proteins in *E. coli* as an experimental model. To minimize the effect of endogenous *E. coli* Bcs complex [31], we deleted *bcsA* in the *E. coli*, which encodes the catalytic subunit of Bcs. Although the deletion of the wider region of the *bcs* gene cluster (e.g. *bcsABZC*) is preferred, we used the *bcsA* deletion mutant in this study because it was difficult to delete even only the *bcsA* gene.

The deletion of the *bcsA* gene in *E. coli* BL21, a strain expressing the Bcs recombinant protein in this study, was performed using the Red/ET recombination system (Gene Bridges GmdH), in which the *bcsA* gene was replaced by the FRT-PGK-gb2-neo-FRT cassette with homology arms of the *bcsA*-flanking region using homologous recombination (Fig. 1A). This genetically modified BL21 (BL21-GM) strain was confirmed by colony direct polymerase chain reaction (PCR) to contain the neomycin resistance gene cassette (FRT-PGK-gb2-neo-FRT cassette; Fig. 1B). When amplified with primer #2 (antibiotic gene cassette specific) and #3 (*E. coli* specific), a band of approximately 1500 bp was found in BL21-GM, while no specific product band was found in wild-type BL21, indicating the insertion of the neomycin resistance gene cassette specifically in BL21-GM. However, when amplified with primers #1 and #3 (either *E. coli*

specific), wild-type BL21 and BL21-GM produced a band corresponding to the *bcsA* gene (2818 bp) and the inserted gene cassette (1731 bp) respectively. These results confirmed the successful deletion of the *bcsA* gene of BL21 in ‘BL21-GM’.

The cellulose-synthesizing activity of BL21-GM was checked *in vivo* by producing DGC fused to thioredoxin (TRX-DGC) in *E. coli* to synthesize c-di-GMP to activate endogenous bacterial cellulose synthase (if there is), as done in our previous study [18] (Fig. 1C). The amounts of cellulose synthesized were approximately 2.3 and 0.7 µg·mL⁻¹ of culture in BL21 and BL21-GM respectively. We assume that the small value obtained for *bcsA*-deleted BL21-GM strain is due to other biopolymers of the extracellular matrix that survived the acid treatment, given that *bcsA* gene was fairly deleted as indicated in Fig. 1B. We then used BL21-GM as a suitable host to express the Bcs subunits with minimal impact on the endogenous Bcs complex of *E. coli*.

Characterization of BsCel5A

Cellulase is an important tool used in this study to scrutinize the role of cellulose molecules in the subunit–subunit interaction of the Bcs complex. In this study, we used a bacterial endo-β-1,4-glucanase from *Bacillus subtilis* (BsCel5A), whose structure has been previously reported [24]. The full length (FL) of this cellulase is a two-domain protein, in which the catalytic domain of GH5 is linked to the carbohydrate-binding module of family 3 (CBM3). In this study, the catalytic domain alone (CD) was also used to maximize access to the soluble substrate. FL and CD of BsCel5A were expressed as glutathione-S-transferase (GST)-fused proteins and purified with glutathione affinity resin, as confirmed by SDS/PAGE (Fig. S1A, left panel). An activity-deficient mutant of E169Q/E257Q in FL (BsCel5A_FL^m) and CD (BsCel5A_CD^m) was also used for a negative control protein in the cellulase treatment experiment.

The binding activity of the purified BsCel5A to phosphoric acid swollen cellulose (PASC) was surveyed to confirm the correct folding of the expressed proteins. The results showed that all the BsCel5A proteins used in this study retained their binding activity to PASC (Fig. S1A, right panel), indicating that all of them were properly folded despite sequence modification. The enzymatic activity of BsCel5A was surveyed to determine whether this cellulase could function at low temperature and neutral pH, which is required for analysing the Bcs complex. Both BsCel5A_FL and BsCel5A_CD hydrolysed barley β-glucan, carboxyl

methyl cellulose (CMC) and PASC at 4 °C and pH 7.5 (Fig. S1B). For Avicel, full-length BsCel5A showed higher activity than the others, stressing the function of CBM to bind solid cellulose.

The substrate specificity of BsCel5A was investigated using cello-oligosaccharides with various degrees of polymerization (DP). BsCel5A hydrolysed cellotetraose, cellopentaose and celohexaose but not cellobiose or cellotriose (Fig. S1C). The final reaction products of BsCel5A for substrates longer than trioses were cellobiose and cellotriose, and the smallest substrate was cellotetraose (Fig. S1D).

Summarizing these, both BsCel5A_FL and BsCel5A_CD were able to hydrolyse cellulose of low crystallinity at 4 °C and pH 7.5, and cellulose molecules with DP higher than three were the substrates. This information was considered when interpreting the data.

Characterization of the Bcs protein complex (1): confirming the function of the recombinant Bcs complex

With the biological resources described in Materials and methods, we analysed the Bcs protein complexes heterogeneously expressed in *E. coli*. Firstly, we checked if the heterogeneously expressed Bcs complexes were functional by using CESEC (cellulose-synthesizing *E. coli*), a platform for estimating the cellulose-synthesizing activity with the co-expression of DGC [18]. All the Bcs complexes expressed in DGC-expressing BL21-GM synthesized a significant amount of cellulose (Fig. 2A), indicating that each of the Bcs complexes expressed in this study is functional, regardless of whether BcsD is tagged. In addition, neither BcsAB nor the BcsABCD complex with the activity-deficient mutant of the catalytic subunit BcsA (D333N or W373A) showed cellulose-synthesizing activity, consistent with our previous study [21]. These results support the idea that the Bcs proteins expressed in this study reflect the state in function and are suitable for an experimental model.

It is notable that the amount of cellulose produced by BcsAB was comparable to that by BcsABCD. However, we do not discuss this observation with regard to the role of the Bcs subunits, given that the cellulose production in this study was measured not *in vitro* but in the living *E. coli* cells, and thus relies on not only the subunit composition but also the physiological state of the cell (e.g. the cytoplasmic concentration of UDP glucose and c-di-GMP).

Despite the lower cellulose production shown in Fig. 2A, we decided to express Bcs proteins without

co-expression of DGC for subsequent purification because higher expression levels of Bcs proteins were detected by WB, as shown in Fig. 2B. As the cellulose quantification in this study used strong acid treatment with acetic acid and nitric acid, we think that highly crystalline cellulose was majorly considered in the data presented in Fig. 2A. Then, it cannot be ruled out that the Bcs complex expressed in *E. coli* without DGC expression synthesizes cellulose.

As observed also in our study for the crude cellulose synthase extracted from *Komagataeibacter xylinus* ATCC53524 [30], the western blot analysis in this study reproducibly showed two bands for BcsA protein: the lower-molecular-weight band around 75 kDa and the higher-molecular-weight band around 250 kDa (Fig. 2B), which account for the monomer and the oligomer of BcsA respectively. Considering the four cellulose chains in the octameric ring structure of BcsD downstream of BcsA [15], the oligomeric band observed in this study may represent the tetrameric BcsA protein, which was stable even in the presence of SDS. Although the oligomeric state of BcsA and its partner BcsB must be evaluated by a suitable method like Blue-Native PAGE in the future, the oligomer band of BcsA in this study was analysed as the indicator for the amount of BcsA protein included in the sample, as well as the monomer band.

Characterization of the Bcs protein complex (2): the complex formation of BcsAB, BcsC and BcsD

Given that BcsD holds the glucan chains in its channel [15], it is functionally located downstream of the BcsAB complex, the core of cellulose molecule synthesis, indicating that BcsD operates in the periplasmic space to assemble cellulose molecules extruded from the BcsAB complex. Furthermore, the BcsC protein has a β -barrel porin-like structure at its C terminus and is supposed to secrete cellulose through the outer membrane [32]. The results from several studies suggest that BcsAB, BcsC and BcsD work together in a coordinated manner to spin bacterial cellulose. We tried to co-express BcsABCD to purify the whole Bcs complex using a hexahistidine tag attached to the C terminus of BcsD (BcsD_{H6}), as the tag at the C terminus does not disturb cellulose-synthesizing activity [16]. All four subunits were successfully purified together by immobilized metal affinity chromatography (IMAC; Fig. 3), while BcsABCD without a tag is not purified in the same condition (Fig. S2), supporting high enough specificity for the hexahistidine-based purification performed in this study. This is the first successful purification of the BcsABCD complex ever reported.

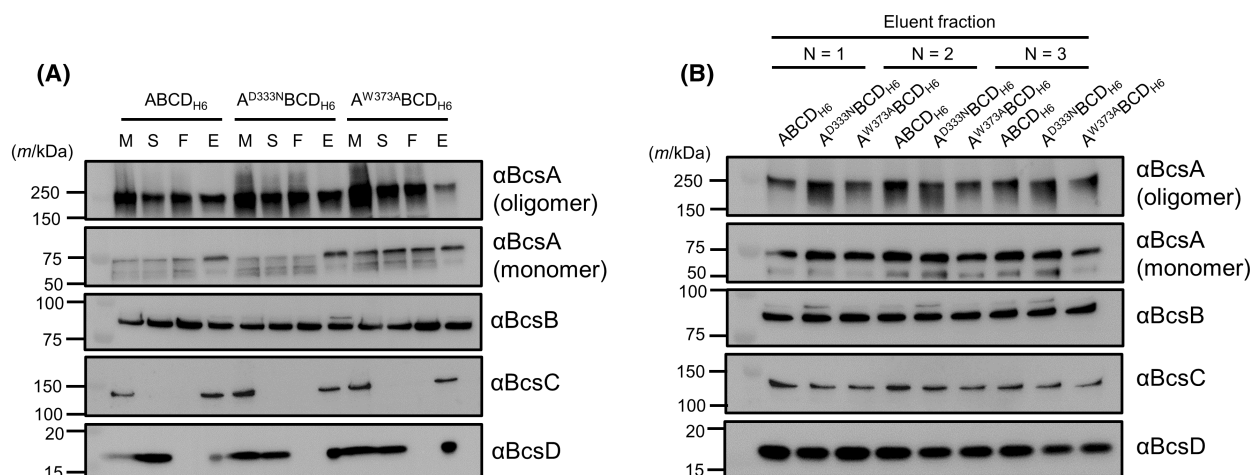


Fig. 3. Purification of BcsABCD_{H6}. (A) WB analysis of the purification process: M, membrane fraction; S, solubilized fraction; F, IMAC unbound fraction; E, IMAC-eluted fraction. Three protein samples, wild-type (BcsABCD_{H6}), D333N on BcsA (BcsA^{D333N}BCD_{H6}) and W373A on BcsA (BcsA^{W373A}BCD_{H6}), were analysed using the antibodies indicated. (B) WB analyses of the eluate from three independent purification experiments for each of the three protein samples. Approximately 2 µg of the protein was loaded onto the gel for WB with BcsA, BcsB and BcsC antibodies, and 1 µg of the protein was added to the gel for WB with BcsD antibody. For BcsA, the data are shown separately for the oligomer and monomer bands.

Yet the quality of this protein purification experiment has to be improved, as no apparent bands for BcsA, BcsB and BcsC were observed in the SDS/PAGE analysis with Coomassie brilliant blue staining (Fig. S3A), despite significant intensity in western blot analysis (Fig. 3). Especially, BcsC was found to be mostly insoluble in detergent (*n*-dodecyl-β-D-maltoside, DDM, in this study) and tended to degrade or aggregate during the purification process (Fig. 3A, BcsC antibody strip), as shown by the lower intensity of the band for BcsC protein (Fig. 3B). We then did not decipher BcsC behaviour in this Bcs complex purification experiment.

Characterization of the Bcs protein complex (3): analysis of the interaction between BcsAB and BcsD by cellulase treatment

As described above, co-expression of BcsABCD_{H6} in *E. coli* allowed the BcsABD complex to be purified reproducibly. Given that BcsABCD_{H6} expressed in *E. coli* is functional as shown in Fig. 2A, we speculated that a glucan chain may link BcsAB and BcsD during this purification. This hypothesis was tested by checking whether the digestion of cellulose resulted in the dissociation of BcsAB from BcsD_{H6} during IMAC purification. BsCel5A cellulase [24], whose mode of action was analysed in this study (Fig. S1), was applied to BcsABCD_{H6} bound to IMAC resin prior to washing and elution. The amounts of BcsA, BcsB, and

BcsD proteins in the eluate were measured by semi-quantitative WB (Fig. 4A); the reliability of quantification in our WB was confirmed, as shown in Fig. S4. The signal intensities of BcsA and BcsB were normalized to that of BcsD in the eluate for comparison between samples. Notably, the amounts of BcsA and BcsB bound to BcsD were decreased by BsCel5A treatment (Fig. 4B), indicating that the BcsAB complex was detached from BcsD by cellulase digestion.

To rule out the possibility that the observed detachment of BcsAB was due to non-specific interaction of the added BsCel5A protein, the activity-deficient mutant of BsCel5A (E169Q/E257Q) was applied to BcsABCD_{H6} bound to the metal affinity resin (Fig. 4C,D). As a result of purification, no decrease in the signal intensity of BcsA and BcsB was observed in the eluate, indicating that cellulose hydrolysis actually caused detachment of BcsAB from BcsD during purification. In summary, the BcsAB complex indirectly interacts with BcsD through the glucan chain.

Two interpretations will be majorly possible for this cellulose-mediated interaction between BcsAB and BcsD protein: (a) the BcsAB and BcsD proteins are non-specifically entangled together with the synthesized cellulose, and (b) the single cellulose chain synthesized by BcsAB complex is specifically trapped by BcsD downstream. If the former interpretation was the case, the treatment by the full-length cellulase (BsCel5A_{FL}) should show similar or even higher efficiency to dissociate BcsAB and BcsD than the catalytic

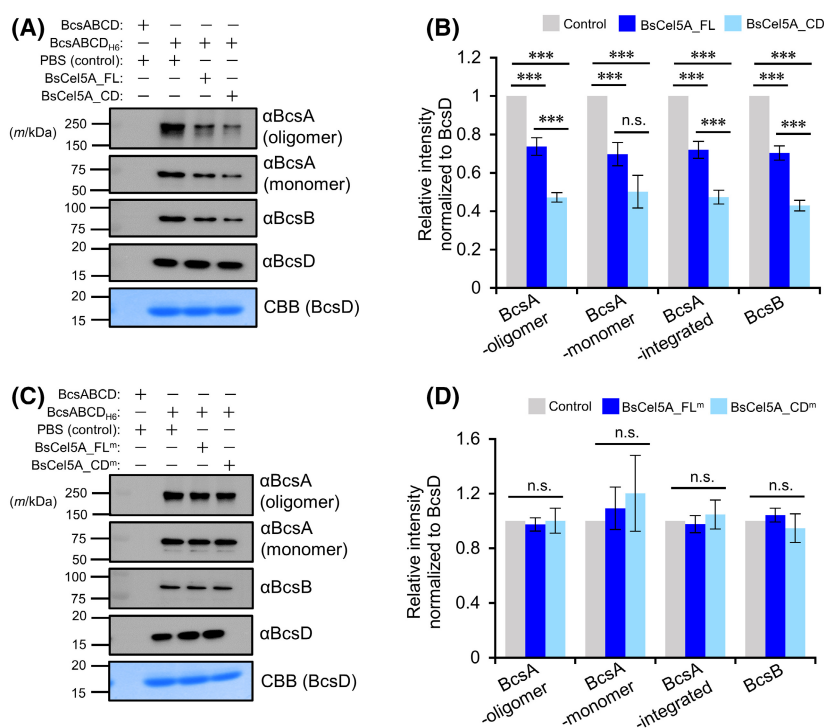


Fig. 4. Effect of cellulase treatment on the purification of Bcs complex. (A) WB images of IMAC-eluted fractions of BcsABCD_{H6} after treatment with wild-type cellulase (BsCel5A_FL and BsCel5A_CD). Coomassie brilliant blue (CBB)-stained images were used as loading controls. (B) Band intensity in WB analysis of (A). Error bars indicate SEM, and the significance of the difference as a result of Student's *t*-test, which was performed using the built-in function of Microsoft Excel (TTEST), is indicated by the symbols: ** for $P < 0.01$, *** for $P < 0.001$ and *n.s.* for not significant ($P > 0.1$). (C) WB images of IMAC-eluted fractions of BcsABCD_{H6} after cellulase mutant (BsCel5A_FL^m and BsCel5A_CD^m) treatment. CBB-stained images were visualized using BcsD as a loading control. (D) Band intensity in WB analysis of (C). Error bars indicate SEM, and Student's *t*-test, which was performed using the built-in function of Microsoft Excel (TTEST), showed no significant difference ($P > 0.1$; eight independent replicates). For BcsA, the data are shown separately for the oligomer band, monomer band and their sum. Each elution sample ($\sim 0.2 \text{ mg}\cdot\text{mL}^{-1}$) was added to an SDS/PAGE gel in 10 μL (anti-BcsA and anti-BcsB) and 1 μL (anti-BcsD and CBB stain) respectively. Elution samples for CBB staining were loaded into gel wells 10-fold more than those for WB (BcsD lane).

domain without CBM (BsCel5A_CD), given the higher activity of BsCel5A_FL to hydrolyse PASC (Fig. S1). However, in fact, the BsCel5A_CD clearly showed a higher performance to dissociate BcsAB and BcsD, as shown in Fig. 3. Then, the former interpretation is not preferable, and we in this study conclude that the cellulose-mediated interaction between BcsAB and BcsD is not non-specific but the specific interaction representing the physiological state of the Bcs complex, as discussed later.

Although cellulase treatment allowed the BcsAB complex to be detached from BcsD during purification, as demonstrated above, a substantial portion of the BcsA and BcsB proteins remained with BcsD in this purification process (Fig. 4B). We supposed that a direct interaction between BcsAB and BcsD is also found in addition to the indirect interaction. To test this hypothesis, we attempted to purify the activity-deficient mutants of BcsABCD_{H6}, BcsA^{D333N}BCD_{H6} and BcsA^{W373A}BCD_{H6}, none of which synthesizes

cellulose, as shown in Fig. 2A. As a result, these mutants allowed BcsA and BcsB to be purified together with BcsD and the wild-type (Fig. 5A,B). Notably, cellulase treatment did not reduce the amount of BcsAB purified together with BcsD for either BcsA^{D333N}BCD_{H6} or BcsA^{W373A}BCD_{H6} (Fig. 5C–E). These results support the existence of direct interaction between BcsAB and BcsD when cellulose is not synthesized. Compiling these cellulase treatment experiments, it was demonstrated that there are two modes of interaction between BcsAB and BcsD: direct and indirect modes through cellulose molecules.

Characterization of the Bcs protein complex (4): pull-down assay to explore the quaternary structure of the Bcs complex

Despite the demonstration of two modes for the interaction between BcsAB and BcsD, the quaternary

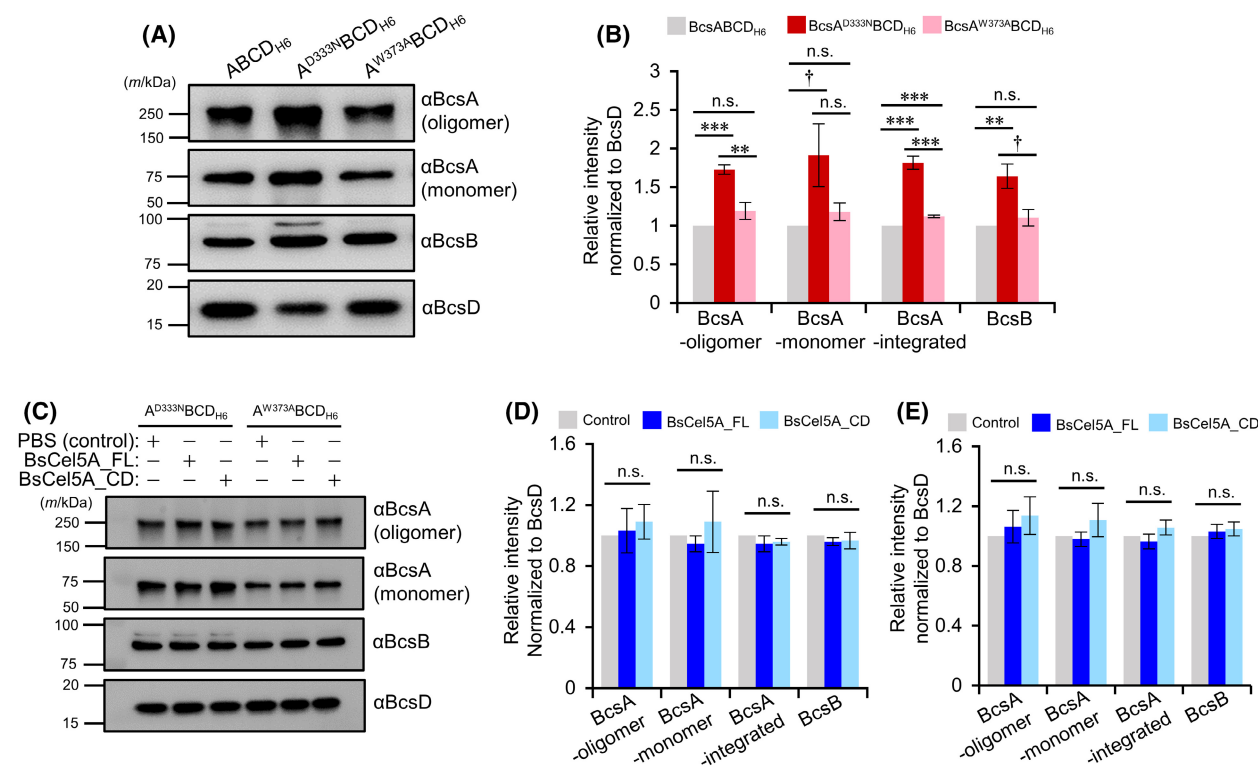


Fig. 5. Effect of cellulase treatment on the purification of mutant Bcs complex. (A) WB images of IMAC-eluted fractions of BcsABCD_{H6}, BcsA^{D333N}BCD_{H6} and BcsA^{W373A}BCD_{H6}. CBB-stained images were visualized using BcsD as a loading control. (B) Band intensity in WB analysis of (A). An error bar indicates SEM, and the significance of the difference as a result of Student's *t*-test, which was performed using the built-in function of Microsoft Excel (TTEST), is indicated by the symbols † for *P* < 0.1, ** for *P* < 0.01, *** for *P* < 0.001 and *n.s.* for not significant (*P* > 0.1). (C) WB images of IMAC-eluted fractions of BcsA^{D333N}BCD_{H6} and BcsA^{W373A}BCD_{H6} after treatment with wild-type cellulase (BsCel5A_FL and BsCel5A_CD). (D, E) Band intensity on WB analysis of (C): (D) for BcsA^{D333N}BCD_{H6} and (E) for BcsA^{W373A}BCD_{H6}. An error bar indicates SEM, and the significance of the difference as a result of Student's *t*-test, which was performed using the built-in function of Microsoft Excel (TTEST), showed no significant difference between any dataset. All experiments were performed with four independent replicates (*n* = 4). For BcsA, the data are shown separately for the oligomer band, monomer band and their sum. Each elution sample (~ 0.2 mg·mL⁻¹) was added to an SDS/PAGE gel in 10 μL (anti-BcsA and anti-BcsB) and 1 μL (anti-BcsD and CBB stain) respectively. Elution samples for CBB staining were loaded into gel wells 10-fold more than those for WB (BcsD lane).

structure of the entire Bcs complex remains to be elucidated. We then performed pull-down assays to further explore the subunit–subunit interactions in the BcsABCD complex by fully utilizing recombinant Bcs proteins. The assay was designed based on the results from previous studies (Fig. 6A): (a) BcsAB forms a complex in the inner membrane [1], (b) BcsC is an outer membrane protein [32,33], (c) BcsD protein is located in the periplasmic space [15,20] and (d) BcsD interacts with the BcsAB complex (this study).

First, the interaction between BcsAB and BcsD, which has been demonstrated above, was tested by pull-down with a bait of Streptag(II)-fused BcsD (BcsD_{StrepII}) and prey of crude BcsAB without tags (DDM-solubilized cell membrane of *E. coli*-expressing BcsAB). As expected, BcsAB bound to BcsD_{StrepII} (Fig. 6B). The pull-down assay yielded a result consistent with our purification experiment of the BcsABD

complex and supported our hypothesis for the interaction between BcsAB and BcsD.

Given the successful pull-down assay with BcsAB and BcsD_{StrepII}, we next performed a pull-down assay to survey the BcsC-involved interaction in the complex (see Fig. 6A). For this purpose, TPR tetratricopeptide-repeat (TPR) domain of the BcsC protein (BcsC_TPR) was used based on two assumptions: (a) the role of the TPR domain is protein–protein interaction [34], and (b) the full-length BcsC protein is unstable, as shown in our purification. Pull-down by BcsD_{StrepII} trapped _{H6}BcsC_TPR_{H6}, which has hexahistidine tags at both the N- and C-termini of BcsC_TPR, in a dose-dependent manner (Fig. 6C), clearly showing that these two proteins interact with each other.

Finally, we performed another two pull-down assays: (a) the purified _{H6}BcsC_TPR_{H6} (bait) with the crude BcsAB (prey; Fig. 6D), and (b) the purified

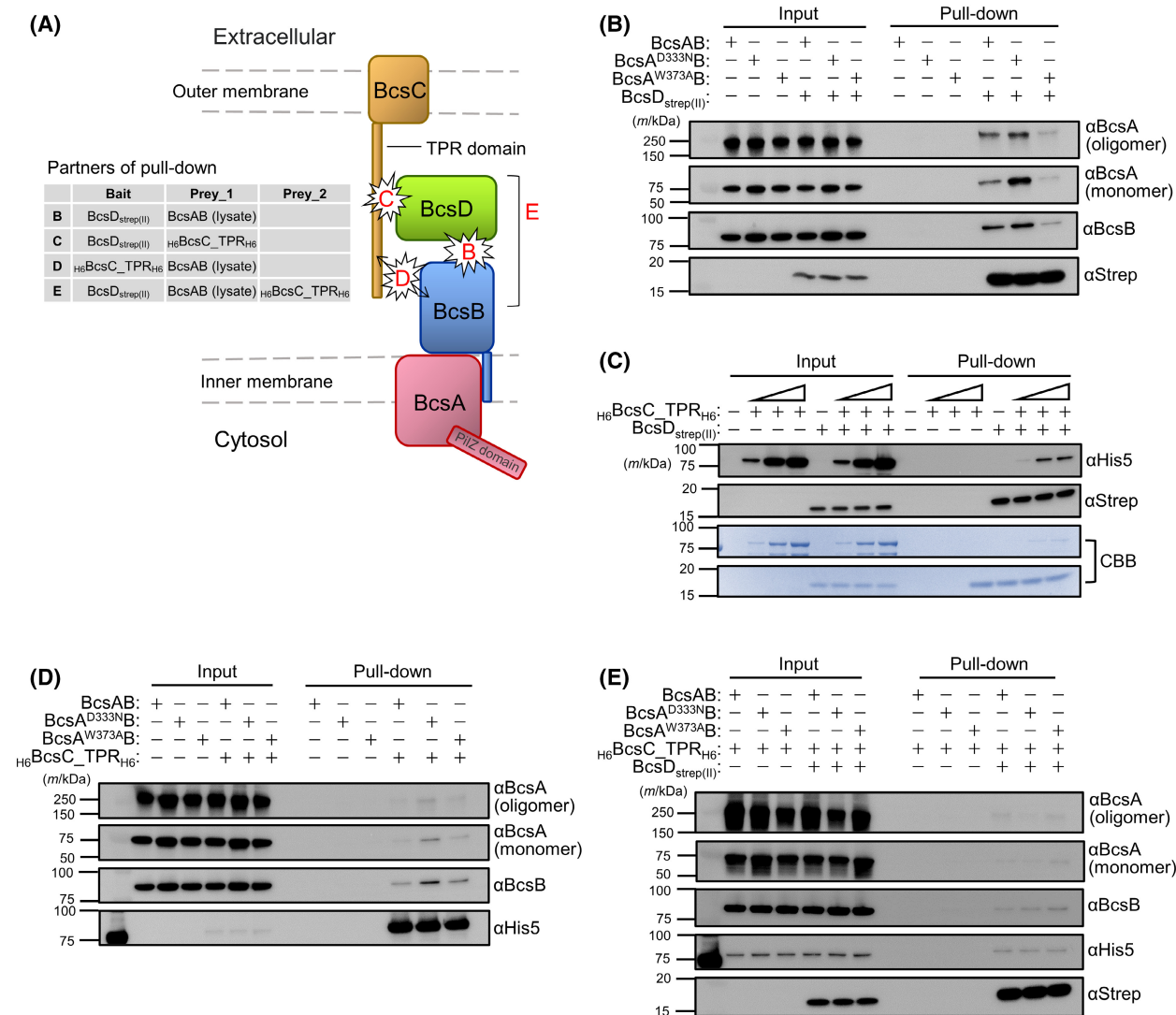


Fig. 6. Pull-down assay with the Bcs subunits. (A) Schematic diagram showing the partners (bait and prey proteins) in a pull-down assay for each subunit of BcsABCD: alphabets on the cartoon indicate the subunit–subunit interactions surveyed in the panels (B–E). (B) WB images of the pull-down assay using BcsD_{strep(II)} (bait) with crude BcsAB (prey). The pull-down fraction was analysed by WB using anti-BcsA, anti-BcsB and anti-Streptag antibodies. (C) WB images of the pull-down assay using BcsD_{strep(II)} (bait) with purified H₆BcsC_TPR_{H6} (prey). The pull-down fraction was analysed by CBB staining and WB using anti-His5 and anti-Streptag antibodies. Input: sample immediately after mixing; pull-down: elution fraction after pull-down. All the detailed methods are described in the ‘Experimental Procedures’ section of the text. Loading factors of H₆BcsC_TPR_{H6} are indicated at the top. (D) WB images of the pull-down assay using H₆BcsC_TPR_{H6} (bait) with crude BcsAB (prey). The pull-down fraction was analysed by WB using anti-BcsA, anti-BcsB and anti-His5 antibodies. (E) WB images of the pull-down assay using BcsD_{strep(II)} (bait) with crude BcsAB (prey_1) and purified H₆BcsC_TPR_{H6} (prey_2). The pull-down fraction was analysed by WB using anti-BcsA, anti-BcsB, anti-His5 and anti-Streptag antibodies. Input: sample immediately after mixing; pull-down: elution fraction after pull-down. All the detailed methods are described in the ‘Experimental Procedures’ section of the text.

BcsD_{strep(II)} (bait) with the crude BcsAB/the purified H₆BcsC_TPR_{H6} mixture (prey; Fig. 6E). The signals on WB in these assays were weak but significant as indicated by no apparent signal in the negative control experiment. Thus, these data support that the subunits of BcsA, BcsB, BcsC and BcsD are contained in the type I Bcs complex.

Discussion

The type I Bcs complex contains the four subunits of BcsA, BcsB, BcsC and BcsD

Bacterial cellulose synthase is a heterosubunit complex. The primary evidence for this hypothesis is the

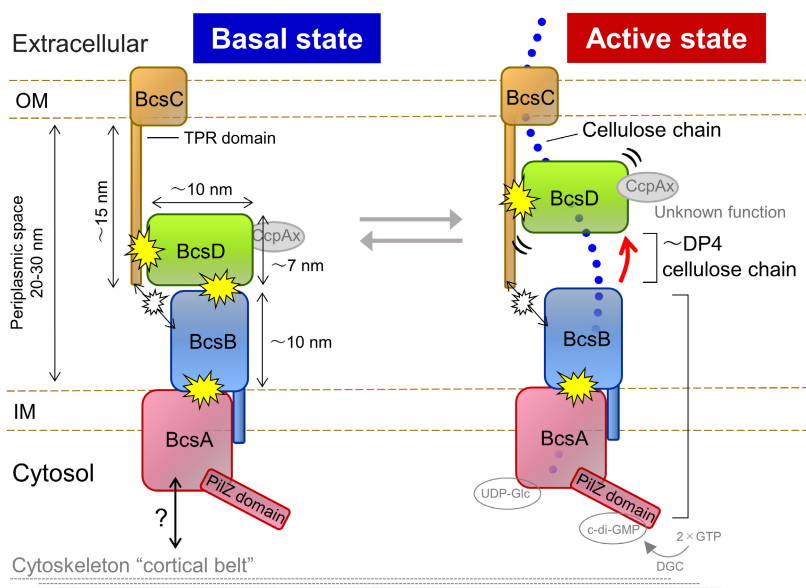


Fig. 7. The hypothetical two-state model for the type I Bcs complex. Hypothetical two-state model for the Bcs complex: basal state (left) and active state (right). In this model, BcsD plays a key role in the periplasmic space to control the state of the complex separately from the state of the BcsA enzyme [1,2]. In the active state (right), BcsD draws the glucan chains in it and brings those chains to the channel pore of BcsC in the outer membrane like a 'button whirligig'. The TPR domain in BcsC may escort the BcsD protein to correctly transfer the glucan chains in BcsD to the BcsC channel. In the basal state (left), BcsD docks with the BcsB complex given that BcsB is located in the periplasmic space [1] as well as BcsD [12,20]. In the model, BcsD in the basal state also docks with BcsC without interfering with BcsB and is ready to draw the glucan chains in it once BcsAB starts synthesizing and extruding out the glucan chain. Thus, BcsD in this state may be a standby state for effectively transferring glucan chains into the extracellular space through the BcsC channel once BcsA is activated. In this cartoon, the subunits that were not assessed in this study are indicated in grey, and the stoichiometry of the subunit composition is not considered for stressing the subunit–subunit interaction.

existence of gene clusters or operons encoding cellulose synthase-related genes [3,6,7,11]. However, this hypothetical model has not been tested intensively, owing to the lack of studies on the protein. Two recent reports have addressed this question. Sunagawa et al. [16] demonstrated an interaction between BcsD and BcsH (Ccp) proteins using a pull-down assay. Another prominent study was the X-ray crystallographic analysis of the BcsAB protein complex by Morgan et al., which clarified that the BcsA and BcsB proteins closely interact with each other to polymerize and translocate the glucan chain from the cytosol to the extracellular side [1], as confirmed also in *E. coli* [35]. In this study, we analysed the type I Bcs complex and demonstrated that the BcsD protein interacted with the BcsAB complex (Figs 3, 4, 5, and 6B) and the TPR domain of BcsC (Fig. 6C). Thus, the co-purification and pull-down assay data in this study indicate that BcsD protein is key to assemble the other three Bcs subunits (BcsA, BcsB and BcsC) to form the Bcs complex. It will be important in the future to clarify the interface of the subunits interacting with each other in the Bcs complex.

However, our co-purification of the BcsABCD complex has an issue of low yield of BcsC protein due to its unsuccessful detergent solubilization and instability, as described in the Result. Although this specific decay of BcsC in the co-purification of BcsABCD is a problem to be fixed, it may indicate that the BcsABD complex can exist stably without BcsC subunit, supporting that the BcsABD complex is the core of the type I Bcs complex *in vivo*. This hypothesis has to be tested in the future.

Dynamic interaction of BcsD protein with BcsAB complex

Interestingly, this study showed that the interaction of BcsD with BcsAB has two modes: direct and indirect interactions through the polymerized glucan chain (Figs 4, 5 and 6). Direct interaction between the BcsAB complex and BcsD protein was observed for both wild-type and catalytically deficient mutant cellulose synthase, whereas the interaction *via* cellulose was observed only for the wild-type (Fig. 5). We then propose a two-state model for the type I Bcs complex:

basal and active states, which are represented by the direct interaction (Fig. 7, left) and indirect interaction modes (Fig. 7, right) respectively.

BcsD protein in this basal state is statically fixed on the BcsAB complex for lying in wait for a glucan chain synthesized by the BcsAB complex. Once cellulose synthesis is initiated, the synthesized glucan chain is guided into the octameric ring of BcsD to crystallize cellulose molecules, as proposed previously [7,15,16,20,36], which is a shift from the resting state to the active state of the complex. In the active state (Fig. 7, right), the BcsD protein is detached from the BcsAB complex but tethered to BcsAB by the glucan chain extruded from BcsAB. Considering that BsCel5A digests the celloglucan longer than DP of 3 (Fig. S1), BcsD can be physically separated from BcsB by a glucan chain with a length of 4 or more glucose residues (Fig. 7).

In this two-state model, the active state of the Bcs complex allows BcsD to be launched towards the outer membrane, while BcsD in the basal state may be fixed statically on BcsB. The TPR domain of the BcsC protein may control diffusible BcsD in the active state in the periplasmic space by gentle but significant interactions. Given that the C-terminal domain of BcsC is an outer membrane β -barrel channel (Fig. S5) [32], the TPR domain of BcsC may escort BcsD carrying glucan chains towards the outer membrane channel in BcsC to spin the glucan chains to the extracellular side. The following questions about this model will be whether (a) BcsD protein could dock to the outer membrane channel part of the BcsC protein and (b) the interaction between BcsC and BcsD could be state dependent. These questions will be addressed in future studies to enhance our understanding of the Bcs complex function.

Conclusion

Our study demonstrated the intermolecular interactions of subunits in the BcsABCD complex to update our knowledge of the quaternary structure of the type I Bcs complex. Experiments in this study were performed using recombinant proteins heterogeneously expressed in *E. coli*; thus, further studies will be necessary to test the hypothesis proposed in this study, the two modes for BcsAB–BcsD interaction: the basal and the active state. Nonetheless, the data obtained in this study were intensively tested using mutagenesis experiments of proteins, and they were consistent with each other. We believe that our hypothesis in this study is sufficiently reliable, at least for starting a further discussion about the mechanism of Bcs with regard to protein function. In this model, BcsD is not statically fixed in the Bcs complex but dynamically interacts

with the other subunits in the complex (Fig. 7). Such a dynamic behaviour may be involved in the crystallization function of cellulose molecules, as well as twisting in bacterial cellulose microfibrils, as reported previously [16]. The putative state control with BcsD, as shown in Fig. 7, is the regulation of the quaternary structure of bacterial cellulose synthase. Next, we need to further study the original *Acetobacter* cells and observe the whole Bcs complex at higher resolution with cryo-EM under controlled two-state conditions.

Acknowledgements

The authors thank Dr Kenji Tajima of Hokkaido University for his advice. The authors thank Professor Ryoichi Yamaji and Dr. Yasuyuki Kobayashi at Osaka Prefecture University for their advice regarding the pull-down assay. This work was supported by JPSP KAKENHI (grant numbers 15H04530 and 19H00950), Exploratory Research on Humanosphere Science (RISH, Kyoto University) and JST CREST (grant number: JPMJCR13B2).

Author contributions

TI and MY conceptualization; TK, TI and MY methodology; TK formal analysis; TK, NY and SN investigation; TI resources; TK and TI data curation; TK and TI writing–original draft; TK, MY and TI writing–review and editing; TK and TI visualization; TI and MY supervision; TK, MY and TI project administration; and TI funding acquisition.

Data availability statement

The data that support the findings of this study are available from the corresponding author [imai.tomoya.4c@kyoto-u.ac.jp] upon reasonable request.

References

- Morgan JLW, Strumillo J, Zimmer J. Crystallographic snapshot of cellulose synthesis and membrane translocation. *Nature*. 2013;**493**:181–6.
- Morgan JLW, McNamara JT, Zimmer J. Mechanism of activation of bacterial cellulose synthase by cyclic di-GMP. *Nat Struct Mol Biol*. 2014;**21**:489–96.
- Römling U, Galperin MY. Bacterial cellulose biosynthesis: diversity of operons, subunits, products, and functions. *Trends Microbiol*. 2015;**23**:545–57.
- Thongsomboon W, Serra DO, Possling A, Hadjineophytou C, Hengge R, Cegelski L.

- Phosphoethanolamine cellulose: a naturally produced chemically modified cellulose. *Science*. 2018;**359**:334–8.
- 5 Tajima K, Imai T, Yui T, Yao M, Saxena I. Cellulose-synthesizing machinery in bacteria. *Cellulose*. 2022;**29**:2755–77.
 - 6 Wong HC, Fear AL, Calhoon RD, Eichinger GH, Mayer R, Amikam D, et al. Genetic organization of the cellulose synthase operon in *Acetobacter xylinum*. *Proc Natl Acad Sci USA*. 1990;**87**:8130–4.
 - 7 Saxena IM, Kudlicka K, Okuda K, Brown RM Jr. Characterization of genes in the cellulose-synthesizing operon (acs operon) of *Acetobacter xylinum*: Implications for cellulose crystallization. *J Bacteriol*. 1994;**176**:5735–52.
 - 8 Standal R, Iversen TG, Coucheron DH, Fjaervik E, Blatny JM, Valla S. A new gene required for cellulose production and a gene encoding cellulolytic activity in *Acetobacter xylinum* are colocalized with the bcs operon. *J Bacteriol*. 1994;**176**:665–72.
 - 9 Kawano S, Tajima K, Kono H, Erata T, Munekata M, Takai M. Effects of endogenous endo- β -1,4-glucanase on cellulose biosynthesis in *Acetobacter xylinum* ATCC23769. *J Biosci Bioeng*. 2002;**94**:275–81.
 - 10 Tajima K, Nakajima K, Yamashita H, Shiba T, Munekata M, Takai M. Cloning and sequencing of the beta-glucosidase gene from *Acetobacter xylinum* ATCC 23769. *DNA Res*. 2001;**8**:263–9.
 - 11 Tonouchi N, Tahara N, Kojima Y, Nakai T, Sakai F, Hayashi T, et al. A beta-glucosidase gene downstream of the cellulose synthase operon in cellulose-producing acetobacter. *Biosci Biotechnol Biochem*. 1997;**61**:1789–90.
 - 12 McNamara JT, Morgan JLW, Zimmer J. A molecular description of cellulose biosynthesis. *Annu Rev Biochem*. 2015;**84**:895–921.
 - 13 Kumagai A, Mizuno M, Kato N, Nozaki K, Togawa E, Yamanaka S, et al. Ultrafine cellulose fibers produced by *Asaia bogorensis*, an acetic acid bacterium. *Biomacromolecules*. 2011;**12**:2815–21.
 - 14 Penttilä PA, Imai T, Capron M, Mizuno M, Amano Y, Schweins R, et al. Multimethod approach to understand the assembly of cellulose fibrils in the biosynthesis of bacterial cellulose. *Cellulose*. 2018;**25**:2771–83.
 - 15 Hu SQ, Gao YG, Tajima K, Sunagawa N, Zhou Y, Kawano S, et al. Structure of bacterial cellulose synthase subunit D octamer with four inner passageways. *Proc Natl Acad Sci USA*. 2010;**107**:17957–61.
 - 16 Sunagawa N, Fujiwara T, Yoda T, Kawano S, Satoh Y, Yao M, et al. Cellulose complementing factor (Ccp) is a new member of the cellulose synthase complex (terminal complex) in *Acetobacter xylinum*. *J Biosci Bioeng*. 2013;**115**:607–12.
 - 17 Omadjela O, Narahari A, Strumillo J, Melida H, Mazur O, Bulone V, et al. BcsA and BcsB form the catalytically active core of bacterial cellulose synthase sufficient for in vitro cellulose synthesis. *Proc Natl Acad Sci USA*. 2013;**110**:17856–61.
 - 18 Imai T, Sun S-j, Horikawa Y, Wada M, Sugiyama J. Functional reconstitution of cellulose synthase in *Escherichia coli*. *Biomacromolecules*. 2014;**15**:4206–13.
 - 19 Du J, Vepachedu V, Cho SH, Kumar M, Nixon BT. Structure of the cellulose synthase complex of *Gluconacetobacter hansenii* at 23.4 Å resolution. *PLoS ONE*. 2016;**11**:e0155886.
 - 20 Sun S-j, Imai T, Sugiyama J, Kimura S. CesaA protein is included in the terminal complex of *Acetobacter*. *Cellulose*. 2017;**24**:2017–27.
 - 21 Sun S-j, Horikawa Y, Wada M, Sugiyama J, Imai T. Site-directed mutagenesis of bacterial cellulose synthase highlights sulfur–arene interaction as key to catalysis. *Carbohydr Res*. 2016;**434**:99–106.
 - 22 Toyosaki H, Naritomi T, Seto A, Matsuoka M, Tsuchida T, Yoshinaga F. Screening of bacterial cellulose-producing *Acetobacter* strains suitable for agitated culture. *Biosci Biotechnol Biochem*. 1995;**59**:1498–502.
 - 23 Nakai T, Moriya A, Tonouchi N, Tsuchida T, Yoshinaga F, Horinouchi S, et al. Control of expression by the cellulose synthase (bcsA) promoter region from *Acetobacter xylinum* BPR 2001. *Gene*. 1998;**213**:93–100.
 - 24 Santos CR, Paiva JH, Sforça ML, Neves JL, Navarro RZ, Cota J, et al. Dissecting structure-function-stability relationships of a thermostable GH5-CBM3 cellulase from *Bacillus subtilis* 168. *Biochem J*. 2012;**441**:95–104.
 - 25 Rao F, Pasunooti S, Ng Y, Zhuo W, Lim L, Liu AW, et al. Enzymatic synthesis of c-di-GMP using a thermophilic diguanylate cyclase. *Anal Biochem*. 2009;**389**:138–42.
 - 26 Cramer A, Whitehorn EA, Tate E, Stemmer WPC. Improved green fluorescent protein by molecular evolution using DNA shuffling. *Nat Biotechnol*. 1996;**14**:315–9.
 - 27 Updegraff DM. Semimicro determination of cellulose in biological materials. *Anal Biochem*. 1969;**32**:420–4.
 - 28 Stahlberg J, Johansson G, Pettersson G. *Trichoderma reesei* has no true exo-cellulase: all intact and truncated cellulase produce new reducing end groups on cellulose. *Biochim Biophys Acta*. 1993;**1157**:107–13.
 - 29 Studier FW. Protein production by auto-induction in high density shaking cultures. *Protein Expr Purif*. 2005;**41**:207–34.
 - 30 Hashimoto A, Shimono K, Horikawa Y, Ichikawa T, Wada M, Imai T, et al. Extraction of cellulose-synthesizing activity of *Gluconacetobacter xylinus* by alkylmaltoside. *Carbohydr Res*. 2011;**346**:2760–8.
 - 31 Acheson JF, Ho RY, Goularte NF, Cegelski L, Zimmer J. Molecular organization of the *E. coli*

- cellulose synthase macrocomplex. *Nat Struct Mol Biol.* 2021;**28**:310–8.
- 32 Acheson JF, Derewenda ZS, Zimmer J. Architecture of the cellulose synthase outer membrane channel and its association with the periplasmic TPR domain. *Structure.* 2019;**27**:1855–61.
- 33 Nojima S, Fujishima A, Kato K, Ohuchi K, Shimizu N, Yonezawa K, et al. Crystal structure of the flexible tandem repeat domain of bacterial cellulose synthesis subunit. *Sci Rep.* 2017;**7**:13018.
- 34 Perez-Riba A, Itzhaki LS. The tetratricopeptide-repeat motif is a versatile platform that enables diverse modes of molecular recognition. *Curr Opin Struct Biol.* 2019;**54**:43–9.
- 35 Abidi W, Zouhir S, Caleechurn M, Roche S, Krasteva PV. Architecture and regulation of an enterobacterial cellulose secretion system. *Sci Adv.* 2021;**7**:eabd8049.
- 36 Uto T, Ikeda Y, Sunagawa N, Tajima K, Yao M, Yui T. Molecular dynamics simulation of cellulose synthase subunit D octamer with cellulose chains from acetic acid bacteria: insight into dynamic behaviors and

thermodynamics on substrate recognition. *J Chem Theory Comput.* 2021;**17**:488–96.

Supporting information

Additional supporting information may be found online in the Supporting Information section at the end of the article.

Appendix S1. Experimental.

Table S1. Primer sequences for gene-disruption using the Red/ET recombination system.

Fig. S1. Characterization of recombinant BsCel5A.

Fig. S2. Selection of affinity resin for BcsABCD copurification.

Fig. S3. Evaluation of the purified BcsABCD proteins by SDS/PAGE with Coomassie brilliant blue staining.

Fig. S4. Quantitative properties of polyclonal Bcs primary antibodies.

Fig. S5. Predicted structure and signal sequence of BcsC.